Nucleic Acids Research, 2005, Vol. 33, No. 17 ***5647–5658***
doi:10.1093/nar/gki876

A new mechanism for mtDNA pathogenesis: impairment of post-transcriptional maturation leads to severe depletion of mitochondrial tRNA$^{Ser(UCN)}$ caused by T7512C and G7497A point mutations

Myriam Möllers[1], Katharina Maniura-Weber[1], Emina Kiseljakovic[1,2], Maria Bust[1], Armine Hayrapetyan[3], Michaela Jaksch[4], Mark Helm[3], Rudolf J. Wiesner[1,5,*] and Jürgen-Christoph von Kleist-Retzow[5,6]

[1]Institute of Vegetative Physiology, University of Köln, Robert-Koch-Strasse 39, 50931 Köln, Germany, [2]Department of Biochemistry, Medical Faculty, Sarajevo, Cekalusa 90, Bosnia and Herzegovina, [3]Institute of Pharmacy and Molecular Biotechnology, University of Heidelberg, Im Neuenheimer Feld 364, 69120 Heidelberg, Germany, [4]Institute of Clinical Chemistry and Mitochondrial Genetics, Kölner Platz 1, 80804 München, Germany, [5]Center for Molecular Medicine Cologne (CMMC), University of Köln, Joseph-Stelzmann-Strasse 52, 50931 Köln, Germany and [6]Department of Pediatrics, University of Köln, Kerpener Strasse 62, 50924 Köln, Germany

Received July 21, 2005; Revised and Accepted September 14, 2005

ABSTRACT

We have studied the consequences of two homoplasmic, pathogenic point mutations (T7512C and G7497A) in the tRNA$^{Ser(UCN)}$ gene of mitochondrial (mt) DNA using osteosarcoma cybrids. We identified a severe reduction of tRNA$^{Ser(UCN)}$ to levels below 10% of controls for both mutations, resulting in a 40% reduction in mitochondrial protein synthesis rate and in a respiratory chain deficiency resembling that in the patients muscle. Aminoacylation was apparently unaffected. On non-denaturating northern blots we detected an altered electrophoretic mobility for G7497A containing tRNA molecules suggesting a structural impact of this mutation, which was confirmed by structural probing. By comparing *in vitro* transcribed molecules with native RNA in such gels, we also identified tRNA$^{Ser(UCN)}$ being present in two isoforms *in vivo*, probably corresponding to the nascent, unmodified transcripts co-migrating with the *in vitro* transcripts and a second, faster moving isoform corresponding to the mature tRNA. In cybrids containing either mutations the unmodified isoforms were severely reduced. We hypothesize that both mutations lead to an impairment of post-transcriptional modification processes, ultimately leading to a preponderance of degradation by nucleases over maturation by modifying enzymes, resulting in severely reduced tRNA$^{Ser(UCN)}$ steady state levels. We infer that an increased degradation rate, caused by disturbance of tRNA maturation and, in the case of the G7497A mutant, alteration of tRNA structure, is a new pathogenic mechanism of mt tRNA point mutations.

INTRODUCTION

Mitochondrial DNA (mtDNA) codes for a total of 37 genes and different human mtDNA alterations, including rearrangements as well as mutations in most of them have been identified as underlying various clinical diseases. In fact, point mutations are responsible for a tremendous number of different clinical phenotypes. This variability has been related to the peculiarities of mitochondrial genetics, e.g. (i) random segregation of a given mutation within the human body, (ii) heteroplasmy, i.e. the coexistence of wild-type and mutated mtDNA molecules within mitochondria, cells and tissues and (iii) threshold effects, meaning that a given mutation becomes

*To whom correspondence should be addressed. Tel: +49 221 478 3610; Fax: +49 221 478 3538; Email: rudolf.wiesner@uni-koeln.de
Present address:
Katharina Maniura-Weber, Empa, Materials Testing and Research, Lerchenfeldstrasse 5, 9014 St Gallen, Switzerland

The authors wish it to be known that, in their opinion, the first two authors should be regarded as joint First Authors

functionally relevant only if it exceeds a certain level of heteroplasmy. However, it has become clear that beyond those characteristics mtDNA point-mutations may have quite variable consequences on the genuine function of the corresponding protein, tRNA or rRNA, and several patterns of those consequences have been identified in the last years (1,2). It is tempting to speculate that these different pathomechanisms not only discriminate, whether a given base pair substitution results in either a functionally irrelevant silent polymorphism or in a potentially disease causing point-mutation, they most likely contribute as well to the quite variable clinical phenotypes of point mutations in any mitochondrial gene. This is particularly true for the 22 tRNA genes where mutations are causing more complex processes than the simple alternative between an either fully functional tRNA or a molecule which is not participating at all in the translational process. Several different pathomechanisms at different levels of cellular function have been identified in the last years: point mutations may reduce the steady state levels of the corresponding tRNA (3), may interfere with the level of aminoacylation with the corresponding amino acid (4), induce an atypical base-modification pattern (5) and may result in quantitative and/or qualitative alterations of protein synthesis and respiratory chain (RC) function (6,7).

Structure, as the basis for all biochemical function, represents a common factor that potentially can be affected by any mutation, and which may have detrimental effects to any number of biochemical interactions. Thus, structural perturbation of tRNAs by pathogenic point mutations represents a potentially significant pathomechanism.

Consequently, structural influence of pathogenic mutation has been investigated in several cases [(8–11), reviewed in (1)]. Because of the central role of tRNAs in protein biosynthesis, and their multiple interactions with a large number of different factors, special considerations are warranted when tRNA structure is examined. Two principle possibilities can be considered: either a mutation does affect the tRNA structure only in the immediate vicinity of the mutation, leaving the general tRNA structure intact, or on the contrary, it severely affects tRNA structure. In the former case, the pathogenic effect is likely to be restricted to the interaction with a single or a few factors, e.g. interfering with aminoacylation if an identity element for tRNA is affected. In the latter case, when the mutated residue represents an important component of tRNA architecture, detrimental effects can be awaited on most of the interactions with other biomolecules. So far, only mild to moderate structural impacts of pathogenic mutations have been described (9). This is not surprising, since serious consequences of significant structural perturbations are likely to cause a strong negative selection pressure on the affected cell.

We have studied the consequences of two pathogenic point mutations (T7512C and G7497A, Supplementary Figure 1) in the $tRNA^{Ser(UCN)}$ gene using osteosarcoma cell cybrids incorporating both mutations at homoplasmic levels and observed that both mutations lead to extremely reduced steady state levels of $tRNA^{Ser(UCN)}$. The biochemical consequences are significant disturbances of mitochondrial protein synthesis and a marked deficiency of complexes I and IV, reproducing the biochemical phenotype in the patients who presented with these mutations which cause serious disease (12). Interestingly, the tRNAs, although present at low levels, are functional regarding aminoacylation in both mutants. Non-denaturing gel electrophoresis comparing *in vitro* transcripts to RNA extracted from cybrids suggests that both mutations lead to a defect of maturation from unmodified to mature tRNA molecules *in vivo*, i.e. a prevailance of degradation over maturation. For the T7512C mutation, a processing defect of a precursor transcript may also be involved.

MATERIALS AND METHODS

Patients

Both patients have already been described (12). In brief, a boy with the G7497A mutation presented at age 3 years with increased exercise intolerance. He showed elevated lactate levels in plasma and cerebrospinal fluid as well as ragged red fibres (RRF) in a muscle biopsy. Meanwhile he developed as well sensorineural deafness. The patient with the T7512C mutation was a boy initially presenting in his first year of life with sensorineural deafness and showing at the age of 6 years myoclonic jerks, dystonic posturing, inability to walk and marked psychomotor retardation including loss of acquired skills. He had no lactic acidosis and no RRF in his muscle biopsy either. Both patients showed a combined RC deficiency of complexes I and IV in muscle (12).

Generation of cybrid cell lines and culture of cells

Cybrid cell lines were constructed by intercellular transfer of patient mtDNA from patient skin fibroblasts to rho^0 143B cells (TK-, subclone rho^0 206) (13). Patient fibroblasts were enucleated using cytochalasin B and then fused with rho^0 cells in the presence of polyethylene glycol. The cybrid cells were cultivated in DMEM containing 4.5 g/l glucose supplemented with 5% fetal calf serum (FCS), Glutamax I, 1 mM sodium pyruvate, 100 μg/ml uridine, 100 U/ml penicillin and 100 μg/ml streptomycin. Single clones were isolated by the cylinder method. For the T7512C mutation a total number of 60 clones, for the G7497A mutation 75 clones were obtained by one fusion experiment.

In order to analyse the rate of degradation of mitochondrial transcripts, 3×10^5 cells were seeded in small dishes, the medium was changed after 24 h and cells were further grown in the presence of ethidium bromide (250 ng/ml) for 24 h or up to 48 h before extraction of RNA. In order to estimate the rates of synthesis of mitochondrial transcripts, cells pre-treated with EtBr for 24 or 48 h were washed extensively to remove the drug and cultivated for another 48 or 96 h.

Fibroblasts of healthy control individuals as well as from both patients were cultivated in RPMI 1640 with Glutamax supplemented with 10% FCS, 200 μM Uridine, 2.5 mM sodium pyruvate, 100 μg/ml Streptomycin and 100 IU/ml Penicillin at 37°C and 5% CO_2.

Validation of the genotype of cybrid clones

In the case of the G7497A mutation, a 926 bp DNA fragment spanning the complete $tRNA^{Ser(UCN)}$ gene was amplified (Supplementary Figure 2A). Within this fragment the G7497A mutation deletes one of two restriction sites for the restriction endonuclease HaeIII. Digestion of the PCR product by HaeIII

yielded a total number of three fragments of the expected size in control samples and in the 143B acceptor cell line, while patient fibroblasts and the all clones showed only two DNA fragments.

Using a similar strategy, a DNA fragment of 175 bp was amplified for the T7512C mutation (Supplementary Figure 2B). The reverse primer introduced by mismatch a novel restriction site for XhoI in the PCR product if derived from the mutated template. Digestion by XhoI yielded only fragments of the predicted smaller size in all clones, while PCR products derived from controls and 143B acceptor cells remained uncut.

Oligonucleotides used for detection of G7497A mutation were: 'mt6961s': ATC GGC ATT GTA TTA GCA AAC, 'mt7887as': CCA ATT GAT TTG ATG GTA AGG and for detection of the T7512C mutation 'mt7375s': ACC TGG AGT GAC TAT ATG GAT G and 'mt7550as': GAC AAA GTT ATG AAA TGG TTT TTC TAA TAC CTT CTC GA.

The nuclear background of all generated cybrid clones was evaluated by amplification of a polymorphic marker on chromosome 11q13 (D11S533) (14) using the following oligonucleotides: 'D11S533s': GCC TAG TCC CTG GGT GTG GTC, 'D11S533as': GGG GGT CTG GGA ACA TGT CCC C.

Oxygen consumption studies and respiratory chain enzyme assays

All cells were grown until they were ~80% confluent. The growth medium was changed the day before harvesting. The final cell pellet contained 10^6–10^7 cells and was resuspended in phosphate-buffered saline (PBS). The resulting cell suspension was then used in part for oxygen consumption studies and was in part frozen for further spectrophotometric assays. The cellular density of the suspension was evaluated by automated counting (CASY, Schärfe Systems, Reutlingen, Germany) while the protein content was determined by Bradford assay (BioRad, München, Germany). Oxygen consumption of intact cells reflecting the metabolism of endogenous substrates was measured within a short and constant time after harvesting using two Clark oxygen electrodes (Hansatech Instruments Limited, King's Lynn, UK). Intact cell respiration was first recorded and then after permeabilization with digitonine the rates for pyruvate (+malate), malate (+glutamate), succinate and glycero-3-phosphate as substrates were determined. Spectrophotometric studies were performed using a Beckmann DU-600 spectrophotometer (Beckmann Instruments, Fullerton, CA) in order to determine the RC enzyme activities of Succinate-cytochrome *c* Reductase (SCCR, complex II and III), Quinol-cytochrome *c* Reductase (QCCR, complex III), cytochrome *c* Oxidase (COX, complex IV) as well as Citrate Synthase (CS) and Lactate Dehydrogenase (LDH) as reference enzymes. Both methods were performed as described in detail (15).

Northern blots

Total RNA was isolated from ~2×10^6 cultured cells using Trizol reagent (Invitrogen, Karlsruhe, Germany).

For the analysis of tRNA levels, synthesis and stability, samples of 0.5 μg total RNA were denatured (100°C for 5 min) and then subjected to electrophoresis through 8% denaturing polyacrylamide gels containing 8 M urea using 1× TBE as gel and running buffer. Separated samples were electroblotted onto Nylon membranes in 0.25× TBE and immobilized by incubation at 80°C for 2 h.

Analysis of precursor transcripts was carried out by separating 3 μg of total RNA through 1.2% agarose gels containing 6.5% formaldehyde and 1× MOPS buffer using 1× MOPS as a running buffer (16). Separated samples were capillary blotted onto Nylon membranes in 10× SSPE and immobilized by incubation at 80°C for 2 h.

For the analysis of tRNA structure, unheated samples of 0.5–3 μg total RNA were subjected to electrophoresis through a 8% non-denaturing polyacrylamide gel using 1× TBE as gel and running buffer. Blotting and immobilization was performed as before.

Aminoacylation levels of tRNAs were analysed under acidic conditions as described previously (17). RNA was isolated using Trizol reagent, however, it was ensured that samples were kept on ice during the procedure and the final RNA pellet was resuspended in 0.3 M sodium acetate (pH 4.5) and 1 mM EDTA. A total of 10 μg of acidic RNA were electrophoresed through a 6.5% acidic denaturing polyacrylamide gel (20 × 43 cm and 1 mm thick) containing 8 M urea and 0.1 M sodium acetate/0.1 M acetic acid (pH 5.0) as running buffer at 4°C and 30 mA over 48 h. Final running distance of xylenecyanol was 23 cm. Deacylation of individual RNA samples was carried out in 0.3 M Tris–HCl (pH 9.0), at 75°C for 15 min. Separated samples were electroblotted and immobilized onto Nylon membranes as described above.

Regions of mtDNA encompassing various mRNA and tRNA genes were used as probes for the northern blots.

Several probes were generated by PCR using the following forward and reverse primers. For ND1: 'mt3384s': AAT TCT AGG CTA TAT ACA AC and 'mt7395as': ATC CAT ATA GTC ACT CCA, which was digested to give specific probes for ND1, ND2 and COI; for ND5/6: 'mt14330s': ACA ACC ACC ACC CCA TCA and 'mt14613as': TCT AAG CCT TCT CCT ATT T; for $tRNA^{Leu(UUR)}$: 'mt3232s': TAA GAT GGC AGA GCC CG and 'mt3305as': TAA TAC GAC TCA CTA TAT TGT TAA GAA GAG GAA TTG; for $tRNA^{Val}$: 'mt1602s': CAG AGT GTA GCT TAA CAC AAA and 'mt1670as': TCA GAG CGG TCA AGT TAA. As template for the PCR reaction DNA derived from 143B control cells was used. PCR products were purified (QIAquick PCR purification columns, Qiagen, Hilden, Germany) and then radiolabelled with [α-^{32}P]dCTP (5000 Ci/mmol) by the random-priming method, while unincorporated nucleotides were removed by gel filtration through ChromaSpin columns (Clontech, Heidelberg, Germany). The probe against the 18S non-mt rRNA was a 5.8 kb insert in pBS-18S released by EcoRI (18) and was labelled as well by random-priming.

5′ end labelling was applied using [γ-^{32}P]ATP (3000 Ci/mmol) for the following probes: for $tRNA^{Ser\ (UCN)}$: 'mt7478s': GGT TTC AAG CCA ACC CCA TGG CCT C; for $tRNA^{Lys}$: 'mt8364as': TCA CTG TAA AGA GGT GTT GGT TCT C; for $tRNA^{Gln}$: 'mt4329s': CTA GGA CTA TGA GAA TCG AA. For the normalization of tRNAs to a non-mtRNA species blots were hybridized with an end-labelled 5S rRNA probe: GGG TGG TAT GGC CGT AGA C (5). Purification and gel filtration was performed for end-labelled probes accordingly.

Hybridization was carried out at 65°C (exceptions: 45°C: $tRNA^{Gln}$; 50°C: ND1, $tRNA^{Ser(UCN)}$; 55°C: $tRNA^{Leu(UUR)}$)

overnight in 10 ml of a solution of 1% SDS, 10% dextran sulfate and 1 M NaCl containing 2×10^6 c.p.m. radiolabelled probe +4 mg sonicated salmon sperm DNA. After hybridization, two 10 min washes were performed at 45° to 65°C with 2× SSC and 0.1% SDS, followed by a 3–10 min wash at 45° to 65°C with 0.1 × SSC, 0.1% SDS. Blots were subjected to PhosphorImager analysis or autoradiography.

Synthesis and structural probing of *in vitro* transcripts

Templates for *in vitro* transcription were amplified by PCR from a synthetic single stranded 144mer DNA encoding a hammerhead ribozyme downstream of a T7-promotor and followed by the sequence of human mt $tRNA^{Ser(UCN)}$ or its respective mutants. Upon transcription with T7-RNA polymerase, the hammerhead ribozyme cleaves at its designated target site to release the tRNA sequence with a 5′-hydroxyl-end (19). After purification over a 12% 8 M urea PAGE, transcripts were passively eluted by agitation in 0.5 M NH_4OAc. 5′-labelling with [γ-^{32}P]ATP and T4-PNK and subsequent purification by PAGE were performed as described (20). 3′-labelling was done by the splint labelling method (21). To detect secondary cleavages, experiments were performed on transcripts labelled on the 5′-extremity, as well as on transcripts labelled on the 3′-extremity. Structural probing with nucleases was done at 35°C as described (20). Since enzyme activities were found to vary greatly over time and among different manufacturers, nuclease concentrations were optimized before every set of experiments, and enzyme dilutions were freshly prepared from stock solutions.

Analysis of mitochondrial protein synthesis

For measurement of protein synthesis, subconfluent cells grown in 12-well plates or 6 cm dishes were washed twice with methionine free medium, then 500 µl or 5 ml, respectively, of methionine free medium containing 10% of dialysed FCS and 100 µg/ml of emetine was added (22) and the incubation was continued for 6 min at 37°C and 5% CO_2. A total of 0.5 mCi of [^{35}S]methionine (Hartmann Analytic, Braunschweig, Germany) were added and the cells were incubated for up to 120 min in initial experiments at 37°C and 5% CO_2. Cells were harvested and labelled protein was precipitated by 10% TCA on glass fiber filters, unincorporated [^{35}S]methionine was removed by extensive washing and incorporation was analysed by liquid scintillation counting (12-well plates). Incorporation into total cell protein in the absence of emetine was linear for 2 h, while incorporation in the presence of emetine increased linearly up to 60 min (data not shown). Thus, measurement of mitochondrial protein synthesis rates was assayed in the following experiments by analyzing the incorporation into mitochondrial proteins after 45 min. For this purpose, cells (6 cm dishes) were lysed in TOTEX buffer [20 mM HEPES (pH 7.9), 400 mM NaCl, 20% Glycerol, 1% NP-40, 1 mM $MgCl_2$, 0.5 mM EDTA, 0.1 mM EGTA, 10 mM β-Glycerophosphate, 10 mM NaF, 5 mM DTT, 0.5 mM Na_3VO_4, and 1 mM PMSF] and labelled proteins were analysed by SDS–PAGE (23). Gels were Coomassie stained, dried and exposed to X-ray films. Autoradiographs were scanned with a densitometer, and the densitometric values obtained for all bands were normalized to the respective values obtained by densitometric scanning of the Coomassie stain.

RESULTS

All generated cybrid clones contain the mutation at homoplasmic level

A considerable number of cybrid clones from either mutation were generated and the mitochondrial genotype of several clones was verified ($n = 15$ for G7497A and $n = 22$ for T7512C). Restriction fragment length analysis showed that all clones, but also the patients fibroblasts were homoplasmic for the two mutations within the detection limits of this method (Supplementary Figure 2A and B).

The complete absence of patient-derived nuclear DNA was confirmed in all clones used for further studies. A polymorphic marker for nuclear DNA D11S533, (14) was amplified and found to be informative: In all 143B control cells, 143B rho^0 acceptor cells and all tested clones amplification yielded only one fragment of a given size while amplification in the two patient fibroblast cell lines yielded one or two fragments, in both cases of a different size. This confirmed successful cybrid generation and homogeneity of 143B-derived nuclear DNA in all clones (Supplementary Figure 2C).

The cybrid clones show a combined deficiency of respiratory chain complexes I and IV like the patients *in vivo*

The biochemical phenotype of the generated cybrid cell lines was then characterized by two different methods. Three different clones were tested for either mutation and compared to 143B cell lines as control. Oxygen consumption of intact cells reflecting the metabolism of endogenous substrates showed a clear decrease in all clones of either mutation (Figure 1A). After permeabilization by digitonin, the oxygen consumption rates of those substrates which feed their electrons into the RC via complex I, i.e. pyruvate (in the presence of malate) and malate (in the presence of glutamate), were likewise clearly decreased. On the other hand, oxygen consumption in the presence of those substrates which feed their electrons distal from complex I into the RC, e.g. succinate and glycero-3-phosphate, via complex II and Glycero-3-Phosphate-Dehydrogenase directly into the pool of quinones respectively, were much less affected compared to controls. This is a clear evidence for a complex I deficiency (15,24). However, as in this experimental setting the activity of COX (complex IV) is not rate-limiting over a considerable range, an additional deficiency of this complex cannot be ruled out based on these results.

Therefore we next performed spectrophotometric assays on the freeze-thawed cell homogenates which were used before in the polarographic studies. We were able to identify a clear COX deficiency in all tested clones of either mutation (Figure 1B). The activities of SCCR (complexes II and III) and of QCCR (complex III) were not significantly reduced when compared to controls, in particular when looking at activity ratios (Figure 1B).

Therefore, in our cybrid cell lines we identified a combined deficiency of complexes I and IV of the respiratory chain by

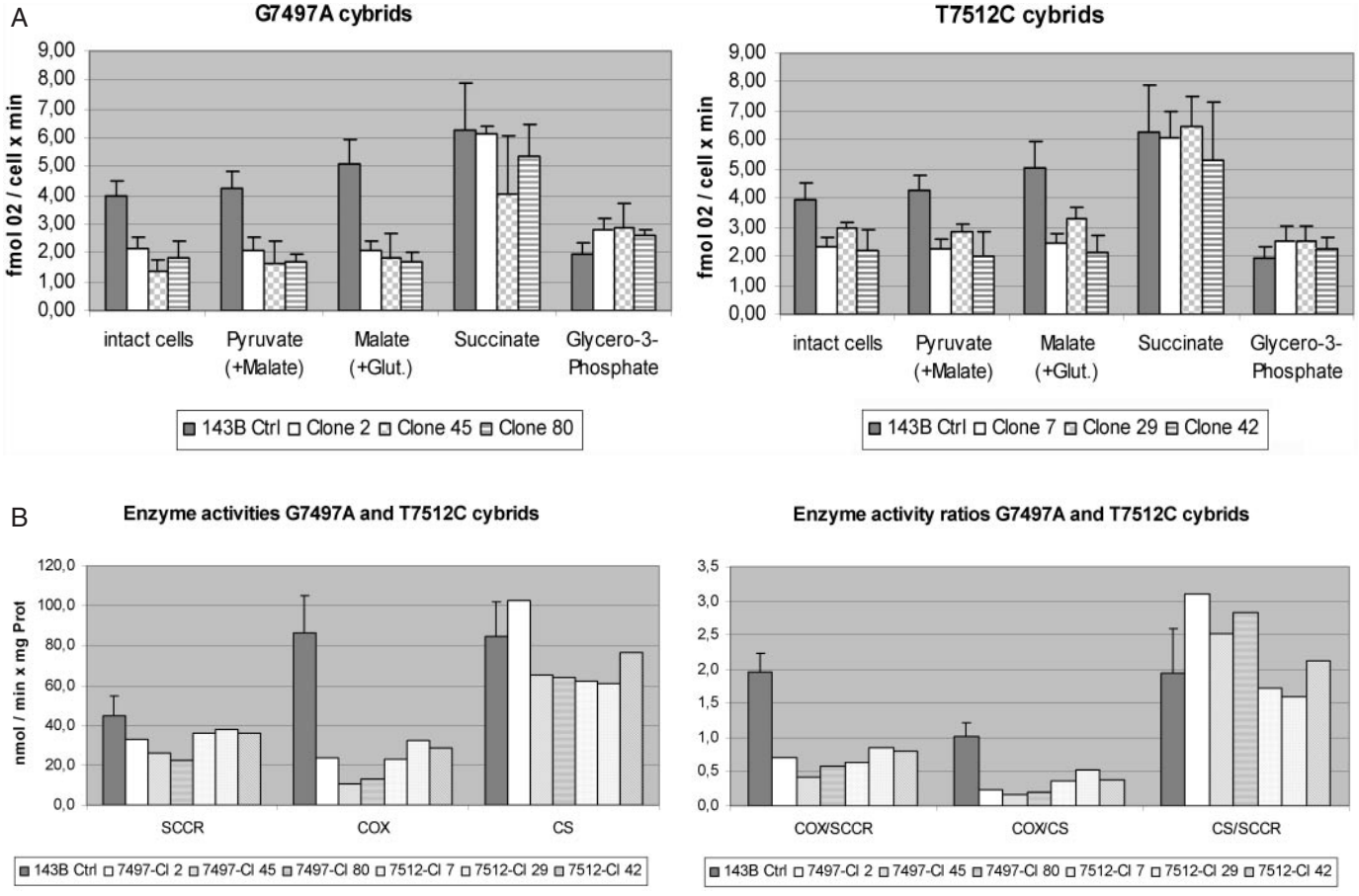

Figure 1. Respiratory chain phenotype of cybrid cell lines. (**A**) Polarography. Graphs show mean values and SDs for oxygen consumption of 143B control cells (solid bars, $n = 10$) and of three different clones containing either mutation (patterned bars, $n \geqslant 3$ for each clone) in intact cells and respiring on indicated substrates after permeabilization. (Glut = glutamate). (**B**) Respiratory chain complex activities. Graphs show SCCR (complex II and III), COX (complex IV) and CS as mitochondrial matrix marker (left panel) and their activity ratios (right panel). Graphs are mean values and SDs for 143B control cells (solid bars, $n = 5$). Enzyme activities were measured only once in each of three different clones containing either mutation.

either mutation, reproducing the biochemical phenotype found in muscle tissue of both patients (12).

Strong reduction of the tRNA$^{Ser(UCN)}$ steady state levels in clones of both mutations

In order to test the potential effects of both mutations on synthesis, stability, structure and function of the tRNA$^{Ser(UCN)}$, a series of northern blots under different electrophoretic conditions was performed.

First, RNA was extracted from cybrid and control cell lines and fractionated on denaturing, urea-containing polyacrylamide gels (Figure 2). Steady state levels of tRNA $^{Ser(UCN)}$ were markedly decreased in all clones of either mutation: when normalized to nuclear encoded 5S rRNA as loading control, steady state levels were calculated to be between 2% (G7497A) and 6% (T7512C) of controls. Steady state levels for tRNA^{Val}, tRNA$^{Leu(UUR)}$ and tRNA^{Gln}, representing other tRNA genes on the heavy and on the light strand, respectively, were found to be unchanged (Figure 2). Moreover, a similar pronounced depletion was detected in RNA samples extracted from fibroblasts of either patient, demonstrating the relevance of our cybrid models for the analysis of the pathogenetic mechanisms of these two mutations.

No accumulation of high molecular weight precursor transcripts

A decreased steady state level of mutated tRNA$^{Ser(UCN)}$ could either result from deficient synthesis of the mtDNA light strand, from a decreased processing rate of larger polycistronic RNA units or from increased degradation of correctly processed but otherwise affected tRNA. To test for abnormal processing, in a first approach we looked for high molecular weight unprocessed intermediates using different double-stranded probes for both, heavy strand and light strand transcripts. Neither ND1 nor ND6/5 probes did reveal different RNA precursors present in either of the clones compared to controls (Figure 3) on these agarose gels. Steady state levels of ND5 and ND1 mRNA were unchanged when compared to 18S rRNA and ND6 mRNA was not visible due to its low abundance. However, we did see low molecular weight unprocessed precursors on non-denaturing PAGE gels in clones harbouring the T7512C mutation (see below).

Synthesis and stability of tRNA$^{Ser(UCN)}$ are not considerably altered by either mutation

We next sought to analyse stability as well as the rate of synthesis of tRNA$^{Ser(UCN)}$. In a first approach, we followed

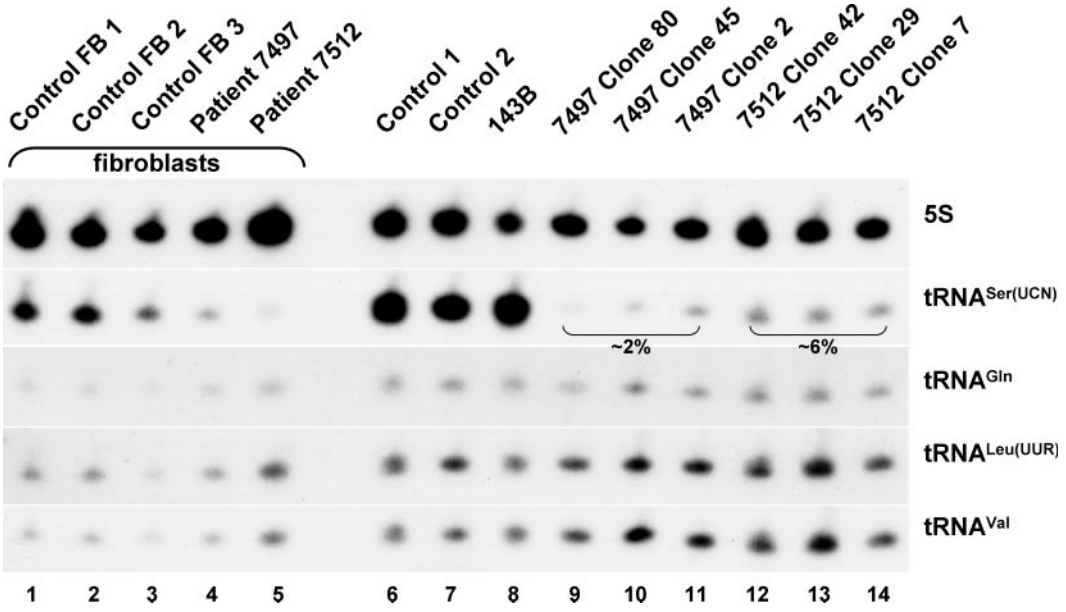

Figure 2. Analysis of tRNA levels by denaturing PAGE and northern blotting. RNA isolated from fibroblasts of both patients and from three healthy controls, from three different cybrid clones containing either mutation as well as from 143B cells and two control cybrid cell lines were run under denaturing conditions, blotted and probed for $tRNA^{Ser\ (UCN)}$, $tRNA^{Gln}$, $tRNA^{Leu(UUR)}$, $tRNA^{Val}$ and for 5S rRNA.

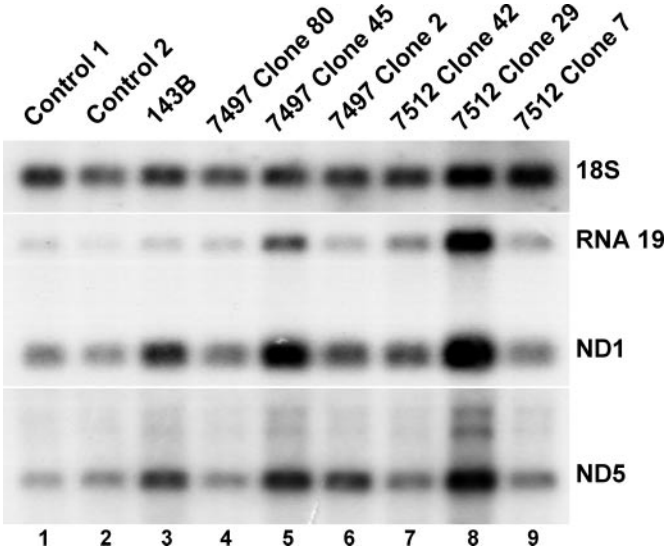

Figure 3. Search for putative precursor transcripts by agarose gel electrophoresis and northern blotting. RNA isolated from three different cybrid clones containing either mutation as well as from 143B cells and two control cybrid cell lines were run, blotted and probed for ND1 and ND5/6 mRNAs as well as for 18S rRNA. Positions of the respective mRNAs as well as the unprocessed precursor transcript RNA19 are given.

the steady state levels over several time points during and after a 48 h period of treatment with ethidium bromide (EtBr), respectively, on denaturing PAGE gels (data not shown). However, due to the very low initial levels the scattering of data precluded the calculation of convincing values for true doubling times or half-lifes of $tRNA^{Ser(UCN)}$, respectively. In a separate set of experiments, stability and synthesis were thus assessed by measuring steady state levels of $tRNA^{Ser(UCN)}$ after a single 24 h period of EtBr treatment and 48 h after withdrawal of EtBr, referring at all time points to the pre-treatment levels (Supplementary Figure 3). Steady state levels of $tRNA^{Ser(UCN)}$ were reduced quite evenly to 57, 67 and 65% of pre-treatment levels for 143B wild-type controls, Clone #2 (7497) and Clone #7 (7512), respectively, after 24 h of treatment. Likewise, we were not able to see major differences in steady state levels reached 48 h after withdrawal of EtBr which were calculated as 67, 75 and 84% for 143B wild-type controls, Clone #2 (7497) and Clone #7 (7512), respectively.

Electrophoretic migration properties of $tRNA^{Ser(UCN)}$ are altered by the G7497 mutation *per se* and suggest defects in post-transcriptional modification

When RNA was run under non-denaturing conditions, we found that the G7497A mutation lead to an acceleration of electrophoretic mobility of $tRNA^{Ser(UCN)}$ (Figure 4A) while the T7512C mutation lead to a rather similar mobility compared to control. Furthermore, all $tRNA^{Ser(UCN)}$ molecules were present in at least two different conformations. These isoforms do not correspond to the acylated and non-acylated forms as the alkaline pH of the gel system used leads to deacylation. Rather, as all examined $tRNA^{Ser(UCN)}$ derivatives display the same electrophoretic mobility in denaturing PAGE systems (Figures 2 and 7), the existence of differently migrating isoforms can be attributed to structural changes induced by post-transcriptional modifications.

In order to investigate whether the mutations alone are sufficient to cause an alteration of electrophoretic mobility and how post-transcriptional modification is involved, *in vitro* $tRNA^{Ser(UCN)}$ transcripts were generated to compare the mobilities of unmodified transcripts with their native, modified counterparts isolated from cybrid cells (Figure 4B). In this blot, only 1/10 of RNA was loaded from control cells in order to facilitate comparison with the much less abundant $tRNA^{Ser(UCN)}$ in cybrid clones. In all cybrid samples two bands

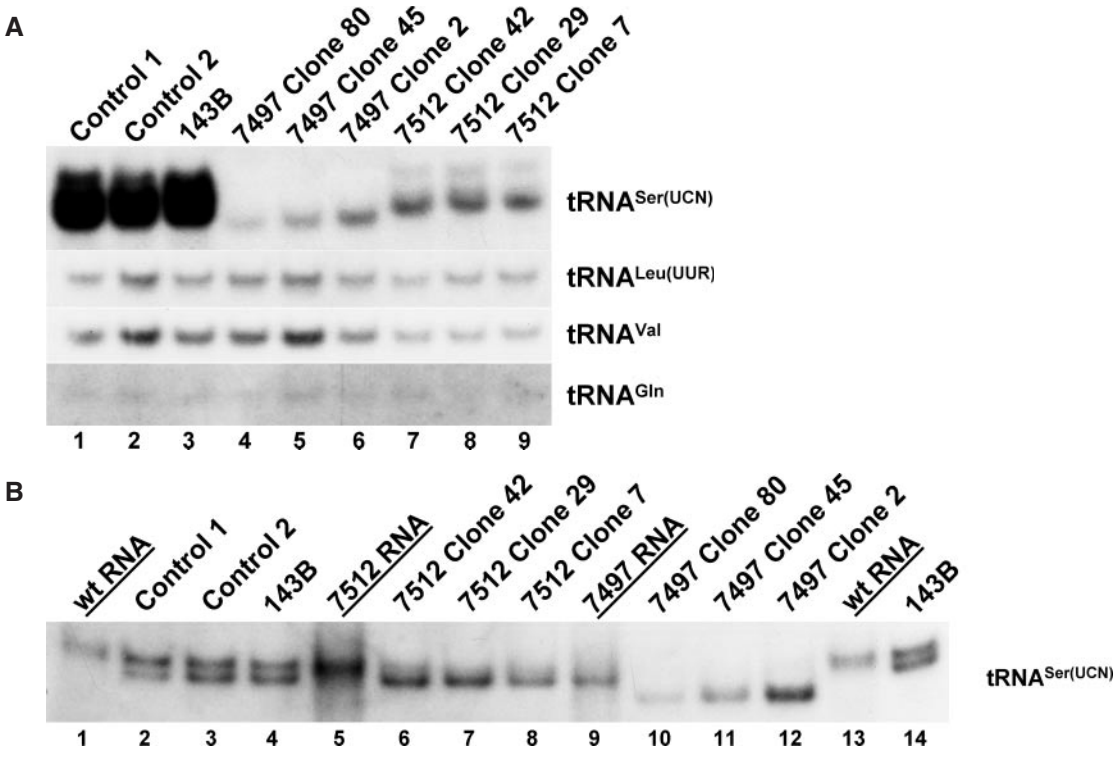

Figure 4. Analysis of tRNA structure by non-denaturing PAGE and northern blotting. (**A**) Cybrid cell RNA. RNA isolated from three different cybrid clones containing either mutation as well as from 143B cells and two control cybrid cell lines were run under non-denaturing conditions, blotted and probed for $tRNA^{Ser(UCN)}$, $tRNA^{Leu(UUR)}$, $tRNA^{Val}$, $tRNA^{Gln}$ and $tRNA^{Lys}$. (**B**) Cybrid cell RNA and *in vitro* transcribed tRNA. RNA samples used in (A) as well as *in vitro* transcribed tRNA (underlined) were run under non-denaturing conditions, blotted and probed for $tRNA^{Ser(UCN)}$. In this blot, only 1/10 of control cell RNA was loaded in order to facilitate comparison of migration with the much less abundant $tRNA^{Ser(UCN)}$ in cybrid clones.

are apparent, albeit the ratio between these bands varied considerably. The upper band displays the same mobility as the respective *in vitro* transcript and hence is considered as being the unmodified (or a partially modified) tRNA. The *in vitro* transcripts, which are cleaved by a ribozyme differ from the *in vivo* tRNAs, besides the absence of modifications, by the lack of a 5′-phosphate group. Thus the mobility of these transcripts were also compared before and after 5′-phosphorylation in a similar gel system and found to be unchanged (Supplementary Figure 4).

The *in vitro* transcripts containing the G7497A mutation migrated faster than transcripts of either wild-type sequence or those containing the T7512C mutation. This indicates that the C to U transition has a noticeable structural impact on the RNA molecule *per se* while the T7512C mutation has no apparent effect.

The second, faster moving band in all native tRNA samples is considered to be the fully modified, mature tRNA. Interestingly, the upper band corresponding to the incompletely modified species is visible, but considerably less abundant in T7512C tRNA and it is present, but barely visible in G7497A tRNA when compared to wild-type controls (Figure 4B). This strongly suggests that both mutations lead to a maturation defect and instability of the unmodified isoform.

In order to support this new concept of several tRNA isoforms existing at detectable levels during the maturation process, we inhibited transcription and thus synthesis of the unmodified isoform by treatment with EtBr and followed recovery after EtBr withdrawal (Figure 5A and B). After 48 h of EtBr treatment (samples labelled 0 h), the mature molecules, although decreased, are clearly more stable than the unmodified species. This can be observed more easily in control cells, but also in the mutant cell lines. During recovery from the treatment, the unmodified species seems to accumulate to higher levels compared to the fully modified at early time points, while the ratio between them is re-established after 72 h of treatment.

Low molecular weight precursor transcripts suggest a processing defect caused by the T7512C mutation

In addition, a similar blot of the same samples as in Figure 4A revealed, after overexposure, several high molecular weight bands hybridizing to the $tRNA^{Ser(UCN)}$ probe (Supplementary Figure 5). These bands were much less abundant than the $tRNA^{Ser(UCN)}$ molecules and were present only in clones containing the T7512C mutation, but undetectable in the clones harbouring the G7497A mutation.

Structural probing reveals mild structural perturbances only in the G7497A mutant

The structural effect of both mutations was investigated more in detail by structural probing. Labelled *in vitro* transcripts were submitted to limited digestion with different nucleases, which are the probes of choice to detect major effects on structure. Figure 6A shows a summary of cleavage patterns

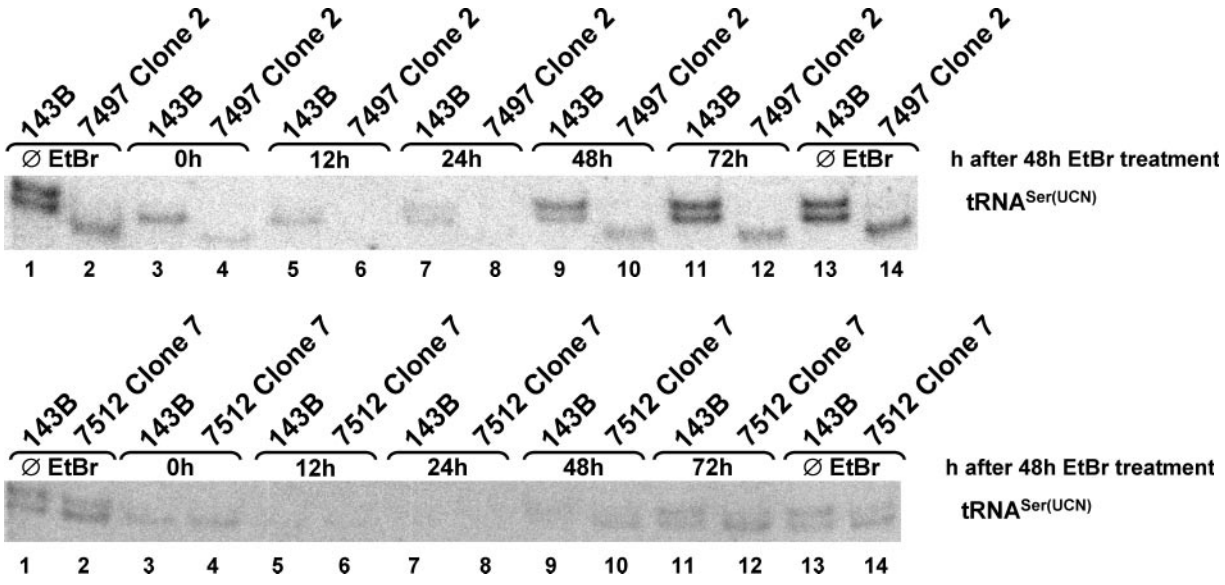

Figure 5. Degradation and synthesis of tRNA species following 48 h of treatment with EtBr and during a 72 h time course after EtBr withdrawal. Levels of tRNA isoforms were analysed by non-denaturing PAGE and northern blotting. Lanes 1 and 2 contain RNA from untreated control (1/10 loaded) and mutant cell line, respectively, 0 h samples were collected after 48 h of EtBr treatment before the recovery experiment started. (**A**) for G7497A mutation (**B**) for T7512C mutation.

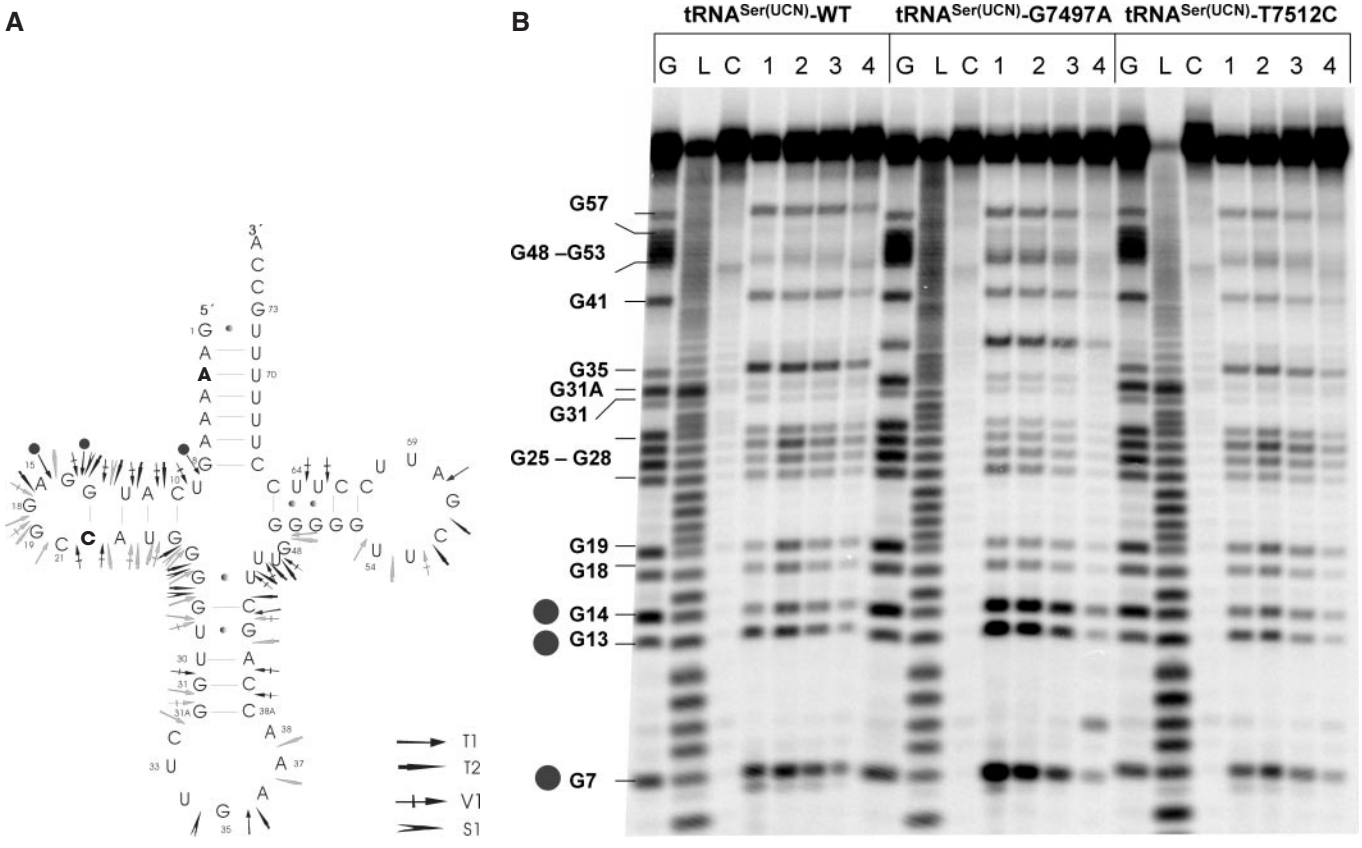

Figure 6. Structural analysis of *in vitro* transcribed tRNAs by limited nuclease digestion. (**A**) Summary of digestion patterns obtained with nucleases T1, T2, V1, S1 for wild-type and tRNA$^{Ser(UCN)}$ transcripts including both mutations (Boldface letters). Arrows indicate the cleavage points on the cloverleaf structure of tRNA$^{Ser(UCN)}$. The darkness of the arrows is proportional to the intensity of cuts, their shape indicate the nuclease used (see inset). Note that the first 5 nt from either end are not included in the analysis for technical reasons. Closed circles indicate differences in intensities of ribonuclease T1 induced cleavages observed in the G7497A mutant. (**B**) Structural probing of wild-type tRNA$^{Ser(UCN)}$ and both mutants. G: ribonuclease T1 cleavage under denaturing conditions; L: alkaline hydrolysis ladder; C: control incubation of refolded tRNA under native conditions; 1–4: limited digestion under native conditions with the decreasing concentrations of ribonuclease T1. Closed circles indicate differences in intensities of ribonuclease T1 induced cleavages observed in the G7497A mutant. Note that the apparent differential migration of the T1 induced cleavage at G35 in the G7497A transcript is an artefact of electrophoresis. The respective bands of 3′-labelled transcripts comigrate at exactly the same level.

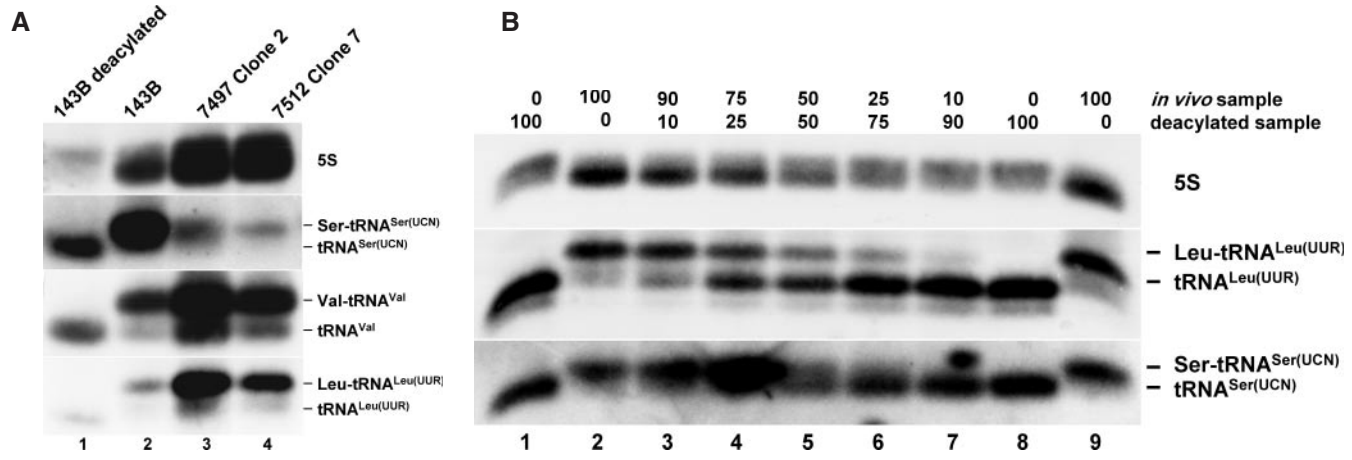

Figure 7. Analysis of aminoacylation of $tRNA^{Ser(UCN)}$ by acidic denaturing PAGE and northern blotting. (**A**) RNA isolated from 143B cells and from one cybrid clone containing either mutation were run under acidic denaturing conditions, blotted and probed for $tRNA^{Ser(UCN)}$, $tRNA^{Val}$, $tRNA^{Leu(UUR)}$ and for 5S rRNA. A sample of deacylated RNA from 143B cells obtained by alkaline treatment was also loaded for comparison. Only 1/5 of RNA was loaded from 143B cells in order to facilitate comparison. (**B**) Mixing experiment using native and deacylated wild-type RNA samples at various ratios. For comparison the blot was probed as well for $tRNA^{Leu(UUR)}$.

obtained with RNases T1, T2 and nucleases S1 and V1 for all transcripts. The cleavage patterns are consistent with the expected cloverleaf structure (25) and the signals obtained with RNases T1 and T2 are generally consistent with those obtained on native fully modified tRNAs using the same probes (11). Surprisingly, the cleavage patterns of the three different transcripts were very similar and no large structural alterations induced by either mutation are apparent from these experiments. A closer investigation of the intensities of cleavages induced by RNase T1 is shown in Figure 6B. Some local changes near the mutation site and the anticodon in transcripts containing the G7497A mutation are detected. These differences, which are indicated by black dots in Figure 6A and B, were apparent in transcripts labelled on either extremity. No significant structural alterations were revealed in *in vitro* transcribed $tRNA^{Ser(UCN)}$ containing the T7512C mutation (Figure 6B). The cleavage patterns obtained with RNAse T2 and ribonucleases V1 and S1 are presented in Supplementary Figure 6.

Mutations do not affect aminoacylation in cybrid cell lines

We investigated the extent of aminoacylation of $tRNA^{Ser(UCN)}$ in cybrid cell lines using high resolution, acid urea PAGE and northern blotting (Figure 7A and B). As control, an aliquot of the 143B RNA-sample was deacylated. All cell lines contain almost exclusively a $tRNA^{Ser(UCN)}$ species migrating clearly slower than the deacylated sample (Figure 7A). In order to estimate the sensitivity of this method, we performed mixing experiments using acylated and deacylated wild-type RNA samples at various ratios (Figure 7B) and find that at least 90% of the tRNA carries the amino acid. We conclude that neither pathogenic mutation has a major detrimental effect on aminoacylation efficiency. Hybridization of the same membranes with probes specific for $tRNA^{Leu(UUR)}$ and $tRNA^{Val}$ (Figure 7A) show that these tRNAs can be more easily separated into their non-acylated and acylated forms, and also that these tRNAs are predominantly charged with amino acids.

Impairment of mitochondrial protein synthesis

Mitochondrial protein synthesis rate was assessed in cybrid cells by pulse labelling with ^{35}S-labelled methionine in the presence of emetine under conditions in which incorporation was linear over time (see Materials and Methods). Mitochondrial proteins in cybrid cells containing either mutation showed a clearly reduced labelling compared to controls (Figure 8A) indicating that protein synthesis rate is slowed down. From a total of four independent experiments we calculated that synthesis rates decreased to 68% and 58% of control for the G7497A and T7512C mutation, respectively (Figure 8B).

DISCUSSION

Pathogenic point mutations in $tRNA^{Ser(UCN)}$ have been identified mainly in patients presenting with isolated deafness. They showed almost invariably high levels of mutant mtDNA, often close to or even reaching homoplasmy, thereby indicating a high threshold for pathogenicity. We have studied in osteosarcoma-derived cybrid cells the consequences of two mutations, G7497A and T7512C, which have been identified in patients with a more complex clinical picture, including exercise intolerance, myoclonus epilepsy and deafness (12). The G7497A mutation was also described in a young girl presenting exclusively with exercise intolerance (26). However, deafness may still develop later in life in this patient, since our patient with this mutation initially also presented with exercise intolerance and fatigue only (12), but became deaf later (unpublished data).

Regarding the responsible pathogenetic mechanisms, we identified as a key finding severely reduced $tRNA^{Ser(UCN)}$ steady state levels below 10% for G7497A and T7512C in osteosarcoma-derived cybrid cells harbouring either mutation at near homoplasmic levels. A comparable marked depletion was evidenced in the patients fibroblasts (Figure 2). Reduced steady state levels are not infrequent in various mutations of mt tRNA genes, but so far, a similar dramatic decrease in

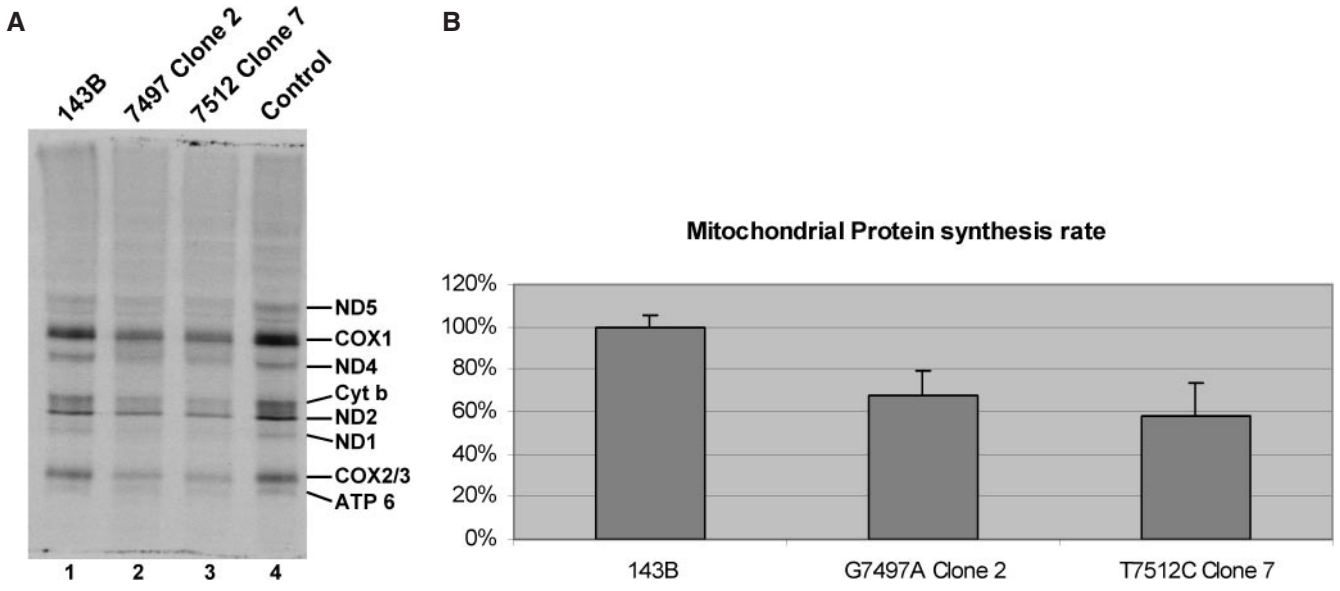

Figure 8. Incorporation of [^{35}S]methionine into mitochondrial proteins. (**A**) Cells were incubated with [^{35}S]methionine for 45 min in the presence of emetine, lysed and protein was separated by SDS–PAGE. Gels were dried and exposed to X-ray film. (**B**) Quantitative evaluation by densitometry of autoradiograms ($n = 4$).

tRNA steady state levels has been reported only in one cybrid model studying a point-mutation in tRNA^{Lys} (27) and—in a clinical context for tRNA^{Val}—in a large family presenting with multiple neonatal deaths (28). It remains puzzling how cells in general and organisms in particular are able to tolerate such a dramatic drop in the level of some mitochondrial tRNAs and, at the same time, retain a basal capacity for protein synthesis, in our cybrid cells still around 60% (Figure 8). Therefore our cell lines make an excellent model system for future studies of mechanisms behind the ability to survive under these conditions, e.g. the stochiometric relationship of components of the mitochondrial translation and protein assembly machinery, the mtDNA haplotype or nuclear modifier genes (29).

There are several reasons why tRNA$^{Ser(UCN)}$ in particular might be at risk for disturbances in processing, degradation and post-transcriptional modification. First, it is the rare example of a 'stranded' gene within the mitochondrial genome (30) as the nearest encoded RNAs are located 7.2 kb upstream and 1.6 kb downstream on the light strand, making the polycistronic precursor transcript very long. This might conceivably commit precursor transcripts to a maturation pathway different from that of heavy strand transcripts, which are tightly packed with transcribed genes. The T7512C mutation is transcribed into an A3G transition at the 5′ end of the tRNA, a location which makes it a likely candidate for misprocessing by mitochondrial RNase P or other processing enzymes. The recognition elements required for processing are poorly characterized, however in analogy with bacterial as well as with eukaryotic RNase P, the 5′ ends of mt tRNAs might contain important recognition signals (31,32). Indeed, light strand transcripts indicative of a possible processing defect of a precursor were detected in cybrid cells containing the T7512C mutation, but not in cells harbouring the G7497A mutation (Supplementary Figure 5). However, they were much less abundant and/or less stable than tRNA$^{Ser(UCN)}$ itself, as was assumed before by Toompuu *et al*. (30). Therefore, this type of processing defect is clearly different from the one seen in patients carrying the A3243G and A3302G mutations in tRNA$^{Leu(UUR)}$ (33–35) and in corresponding cybrid models (K. Maniura-Weber and R. J. Wiesner, unpublished data), in which the heavy strand precursor RNA19 accumulates to high abundance.

Second, tRNA$^{Ser(UCN)}$ has an unusual structure with a short connector region between the acceptor stem and the D-stem, a relatively small D-loop, a 3 nt short variable loop and a long 6 bp anticodon stem [see (36) and (1) for a review on mt tRNA structure]. The A3G transition resulting from the T7512C mutation changes the wild-type A-U into a G-U base pair within the acceptor stem, which however affects stability only marginally. According to present knowledge on tRNA structure, this change should at most induce a slight kink in the acceptor helix, which is indeed consistent with our structural probing data (Figure 6). The G7497A mutation results in a C22U transition and an ensuing G-U base pair in the D-stem. This is in close proximity to the two guanosines at positions 18 and 19, which form tertiary D-loop–T-loop interactions (37,38) similar to those in cytosolic tRNAs. The mutation might thus subtly influence the strength of these tertiary interactions. Interestingly, a potentially similar situation has been recently described for tRNA$^{Leu(CUN)}$, where two alternative T-stem alignments were found which may influence the same set of tertiary interactions (39). Variations in those same tertiary interactions in cytosolic tRNAs are known to affect the angle between acceptor stem and anticodon stem and have been experimentally shown to affect migration behaviour in non-denaturing gels (40). This is at present the most plausible hypothesis to account for the differential migration behaviour displayed by the investigated tRNAs in such gels. Indeed, non-denaturing gel electrophoresis of both, native tRNA and *in vitro* transcripts, shows that the G7497A mutation induces a structural change *per se*, namely a compaction leading to faster electrophoretic mobility, while T7512C does not (Figure 4B). Furthermore, this gel system identifies two tRNA species present in cybrid cells, namely a slow migrating

population co-migrating with the corresponding *in vitro* transcripts and a second, faster migrating population. These probably correspond to unmodified (or partially modified) molecules and mature tRNAs, respectively, which are the fully modified molecules, at least in wild-type cells. In all cell lines, post-transcriptional modification leads to structural compaction enhancing the mobility of the maturated tRNA to about the same extent. Indeed, inhibition of *de novo* synthesis of tRNAs by EtBr and release of this inhibition supports this concept of a pool of unmodified tRNAs being converted into the more stable, fully modified molecules (Figure 5A and B).

The identity of the base modifications responsible for compaction of the structure of $tRNA^{Ser(UCN)}$ needs to be elucidated in further studies. Native human mt $tRNA^{Ser(UCN)}$ contains four different modified nucleotides at five positions in the tRNA structure (11). Because of their location in the structural core, the pseudouridines 27 and 55 and ribothymidine 54 are the most likely candidates to effect a structural rearrangement as evidenced in our non-denaturing PAGE experiments.

Furthermore, the ratio between unmodified and maturated populations is clearly altered in the clones incorporating both mutations. While wild-type cells contain rather similar amounts of both, the T7512C clones show preferentially, the G7497A clones almost exclusively the faster migrating isoform (Figure 4B). The amount of fully modified tRNAs most likely is the result of a competition between maturation by modifying enzymes and degradation by nucleases. We hypothesize that both mutations lead to an impairment of post-transcriptional modification processes, ultimately leading to a preponderance of degradation over maturation (41). Consequently, the levels of maturated $tRNA^{Ser(UCN)}$ molecules are severely decreased.

However, the maturated $tRNA^{Ser(UCN)}$ populations show no major impairment of aminoacylation (Figure 7A). The second serine isoacceptor in the mammalian mitochondrial genome, $tRNA^{Ser(AGY)}$ does not contain a D-domain. Furthermore, it does not share any significant sequence homologies with its counterpart $tRNA^{Ser(UCN)}$, which raised the question how the single mitochondrial seryl-tRNA synthetase (SerRS) recognizes both of its cognate tRNAs. The T-domain was identified as the region containing the major identity elements required for tRNA serylation (42,43). The investigated mutations T7512C and G4797A give rise to transitions A3G and C22U, both of which are too remote from that domain to significantly affect aminoacylation. According to previous investigations (43), the structural effect of the C22U mutation on the tertiary interactions between D-loop and T-loop might lead to a secondary impairment on aminoacylation. However our *in vivo* data show no such evidence.

A number of studies have been devoted to investigate the effects of pathogenic mutations on processing of mt tRNA precursors and on aminoacylation using both, *in vitro* synthesized tRNA and purified enzymes as well as cybrid cell lines (30,44–46). So far, investigations regarding post-transcriptional nucleotide modification mostly focused on wobble-base modifications in the anticodon loop, which affect mRNA decoding (5,47,48). However, little attention has been paid to maturation processes affecting tRNA structure and its stability as a consequence of post-transcriptional modifications. The present work establishes such a connection by presenting a set of experimental data, which link structural disturbance, post-transcriptional modification events and a high degree of tRNA instability in two $tRNA^{Ser(UCN)}$ mutations. Precise details of the pathogenic pathway of the T7512C mutation remain to be further elucidated. The corresponding cybrid cell lines make well suited models in further detailed investigations to distinguish the factors discussed above as causes and consequences in pathogenesis as well as for the further study of mt tRNA stability and modification.

In summary, our cybrids show that both mutations cause an impairment of post-transcriptional maturation, leading to an accelerated degradation of unmodified or partially modified tRNAs. The T7512C mutation seems to cause an additional processing defect, which could alone explain the low steady state of the mature tRNA, but not the altered ratio between the isoforms. These mechanisms lead to severely reduced steady state levels of aminoacylated $tRNA^{Ser(UCN)}$, causing a considerable decrease of mitochondrial protein synthesis rate, finally resulting in a severe biochemical defect of respiratory chain function.

SUPPLEMENTARY DATA

Supplementary Data are available at NAR Online.

ACKNOWLEDGEMENTS

Supported by the Köln Fortune Program, Faculty of Medicine, University of Köln (J.C.v.K.R. and M.B.), Fritz-Thyssen-Stiftung (K.M.W. and M.M.) and Deutsche Forschungsgemeinschaft (Ja 802/2-1, M.J. and HE 3397/3, M.H.). We would like to thank Dr M. King for the generous gift of 143B (TK^-) wild-type and 143B (rho^0 206) cells. Funding to pay the Open Access publication charges for this article was provided by Center for Molecular Medicine Cologne (CMMC).

Conflict of interest statement. None declared.

REFERENCES

1. Florentz,C., Sohm,B., Tryoen-Toth,P., Putz,J. and Sissler,M. (2003) Human mitochondrial tRNAs in health and disease. *Cell Mol. Life Sci.*, **60**, 1356–1375.
2. Florentz,C. and Sissler,M. (2001) Disease-related versus polymorphic mutations in human mitochondrial tRNAs. Where is the difference? *EMBO Rep.*, **2**, 481–486.
3. Chomyn,A., Enriquez,J.A., Micol,V., Fernandez-Silva,P. and Attardi,G. (2000) The mitochondrial myopathy, encephalopathy, lactic acidosis, and stroke-like episode syndrome-associated human mitochondrial tRNALeu(UUR) mutation causes aminoacylation deficiency and concomitant reduced association of mRNA with ribosomes. *J. Biol. Chem.*, **275**, 19198–19209.
4. El Meziane,A., Lehtinen,S.K., Holt,I.J. and Jacobs,H.T. (1998) Mitochondrial tRNALeu isoforms in lung carcinoma cybrid cells containing the np 3243 mtDNA mutation. *Hum. Mol. Genet.*, **7**, 2141–2147.
5. Yasukawa,T., Suzuki,T., Ueda,T., Ohta,S. and Watanabe,K. (2000) Modification defect at anticodon wobble nucleotide of mitochondrial tRNAs(Leu)(UUR) with pathogenic mutations of mitochondrial myopathy, encephalopathy, lactic acidosis, and stroke-like episodes. *J. Biol. Chem.*, **275**, 4251–4257.
6. Dunbar,D.R., Moonie,P.A., Zeviani,M. and Holt,I.J. (1996) Complex I deficiency is associated with 3243G:C mitochondrial DNA in osteosarcoma cell cybrids. *Hum. Mol. Genet*, **5**, 123–129.

7. El Meziane,A., Lehtinen,S.K., Hance,N., Nijtmans,L.G., Dunbar,D., Holt,I.J. and Jacobs,H.T. (1998) A tRNA suppressor mutation in human mitochondria. *Nature Genet*, **18**, 350–353.
8. Wittenhagen,L.M., Roy,M.D. and Kelley,S.O. (2003) The pathogenic U3271C human mitochondrial tRNA(Leu(UUR)) mutation disrupts a fragile anticodon stem. *Nucleic Acids Res.*, **31**, 596–601.
9. Wittenhagen,L.M. and Kelley,S.O. (2003) Impact of disease-related mitochondrial mutations on tRNA structure and function. *Trends Biochem. Sci.*, **28**, 605–611.
10. Sohm,B., Frugier,M., Brule,H., Olszak,K., Przykorska,A. and Florentz,C. (2003) Towards understanding human mitochondrial leucine aminoacylation identity. *J. Mol. Biol*, **328**, 995–1010.
11. Toompuu,M., Yasukawa,T., Suzuki,T., Hakkinen,T., Spelbrink,J.N., Watanabe,K. and Jacobs,H.T. (2002) The 7472insC mitochondrial DNA mutation impairs the synthesis and extent of aminoacylation of tRNASer(UCN) but not its structure or rate of turnover. *J. Biol. Chem.*, **277**, 22240–22250.
12. Jaksch,M., Klopstock,T., Kurlemann,G., Dorner,M., Hofmann,S., Kleinle,S., Hegemann,S., Weissert,M., Muller-Hocker,J., Pongratz,D. *et al.* (1998) Progressive myoclonus epilepsy and mitochondrial myopathy associated with mutations in the tRNA(Ser(UCN)) gene. *Ann. Neurol.*, **44**, 635–640.
13. King,M.P. and Attardi,G. (1989) Human cells lacking mtDNA: repopulation with exogenous mitochondria by complementation. *Science*, **246**, 500–503.
14. Eubanks,J.H., Selleri,L., Hart,R., Rosette,C. and Evans,G.A. (1991) Isolation, localization, and physical mapping of a highly polymorphic locus on human chromosome 11q13. *Genomics*, **11**, 720–729.
15. Rustin,P., Chretien,D., Bourgeron,T., Gerard,B., Rotig,A., Saudubray,J.M. and Munnich,A. (1994) Biochemical and molecular investigations in respiratory chain deficiencies. *Clin. Chim. Acta.*, **228**, 35–51.
16. Sambrook,J., Fritsch,E.F. and Maniatis,T. (1989) *Molecular Cloning: A Laboratory Manual*. Cold Spring Harbor Laboratory Press, USA.
17. Yasukawa,T., Suzuki,T., Ishii,N., Ohta,S. and Watanabe,K. (2001) Wobble modification defect in tRNA disturbs codon-anticodon interaction in a mitochondrial disease. *EMBO J.*, **20**, 4794–4802.
18. Wilson,G.N., Hollar,B.A., Waterson,J.R. and Schmickel,R.D. (1978) Molecular analysis of cloned human 18S ribosomal DNA segments. *Proc. Natl Acad. Sci. USA*, **75**, 5367–5371.
19. Fechter,P., Rudinger,J., Giege,R. and Theobald-Dietrich,A. (1998) Ribozyme processed tRNA transcripts with unfriendly internal promoter for T7 RNA polymerase: production and activity. *FEBS Lett.*, **436**, 99–103.
20. Helm,M., Brule,H., Degoul,F., Cepanec,C., Leroux,J.P., Giege,R. and Florentz,C. (1998) The presence of modified nucleotides is required for cloverleaf folding of a human mitochondrial tRNA. *Nucleic Acids Res.*, **26**, 1636–1643.
21. Huang,Z. and Szostak,J.W. (1996) A simple method for 3′-labeling of RNA. *Nucleic Acids Res.*, **24**, 4360–4361.
22. Chomyn,A. (1996) *In vivo* labeling and analysis of human mitochondrial translation products. *Methods Enzymol.*, **264**, 197–211.
23. Laemmli,U.K. (1970) Cleavage of structural proteins during the assembly of the head of bacteriophage T4. *Nature*, **227**, 680–685.
24. Hofhaus,G., Shakeley,R.M. and Attardi,G. (1996) Use of polarography to detect respiration defects in cell cultures. *Methods Enzymol.*, **264**, 476–483.
25. Yokogawa,T., Watanabe,Y., Kumazawa,Y., Ueda,T., Hirao,I., Miura,K. and Watanabe,K. (1991) A novel cloverleaf structure found in mammalian mitochondrial tRNA(Ser) (UCN). *Nucleic Acids Res.*, **19**, 6101–6105.
26. Grafakou,O., Hol,F.A., Otfried,S.K., Siers,M.H., ter Laak,H., Trijbels,F., Ensenauer,R., Boelen,C. and Smeitink,J. (2003) Exercise intolerance, muscle pain and lactic acidaemia associated with a 7497G>A mutation in the tRNASer(UCN) gene. *J. Inherit. Metab. Dis.*, **26**, 593–600.
27. Bacman,S.R., Atencio,D.P. and Moraes,C.T. (2003) Decreased mitochondrial tRNALys steady-state levels and aminoacylation are associated with the pathogenic G8313A mitochondrial DNA mutation. *Biochem. J.*, **374**, 131–136.
28. McFarland,R., Clark,K.M., Morris,A.A., Taylor,R.W., Macphail,S., Lightowlers,R.N. and Turnbull,D.M. (2002) Multiple neonatal deaths due to a homoplasmic mitochondrial DNA mutation. *Nature Genet.*, **30**, 145–146.
29. Toompuu,M., Tiranti,V., Zeviani,M. and Jacobs,H.T. (1999) Molecular phenotype of the np 7472 deafness-associated mitochondrial mutation in osteosarcoma cell cybrids. *Hum. Mol. Genet.*, **8**, 2275–2283.
30. Toompuu,M., Levinger,L.L., Nadal,A., Gomez,J. and Jacobs,H.T. (2004) The 7472insC mtDNA mutation impairs 5′ and 3′ processing of tRNA(Ser(UCN)). *Biochem. Biophys. Res. Commun.*, **322**, 803–813.
31. Frank,D.N. and Pace,N.R. (1998) Ribonuclease P: unity and diversity in a tRNA processing ribozyme. *Annu. Rev. Biochem.*, **67**, 153–180.
32. Christian,E.L., Zahler,N.H., Kaye,N.M. and Harris,M.E. (2002) Analysis of substrate recognition by the ribonucleoprotein endonuclease RNase P. *Methods*, **28**, 307–322.
33. Bindoff,L.A., Howell,N., Poulton,J., McCullough,D.A., Morten,K.J., Lightowlers,R.N., Turnbull,D.M. and Weber,K. (1993) Abnormal RNA processing associated with a novel tRNA mutation in mitochondrial DNA. A potential disease mechanism. *J. Biol. Chem.*, **268**, 19559–19564.
34. Kaufmann,P., Koga,Y., Shanske,S., Hirano,M., DiMauro,S., King,M.P. and Schon,E.A. (1996) Mitochondrial DNA and RNA processing in MELAS. *Ann. Neurol.*, **40**, 172–180.
35. Koga,A., Koga,Y., Akita,Y., Fukiyama,R., Ueki,I., Yatsuga,S. and Matsuishi,T. (2003) Increased mitochondrial processing intermediates associated with three tRNA(Leu(UUR)) gene mutations. *Neuromuscul. Disord.*, **13**, 259–262.
36. Helm,M., Brule,H., Friede,D., Giege,R., Putz,D. and Florentz,C. (2000) Search for characteristic structural features of mammalian mitochondrial tRNAs. *RNA*, **6**, 1356–1379.
37. Watanabe,Y., Kawai,G., Yokogawa,T., Hayashi,N., Kumazawa,Y., Ueda,T., Nishikawa,K., Hirao,I., Miura,K. and Watanabe,K. (1994) Higher-order structure of bovine mitochondrial tRNA(SerUGA): chemical modification and computer modeling. *Nucleic Acids Res.*, **22**, 5378–5384.
38. Hayashi,I., Kawai,G. and Watanabe,K. (1998) Higher-order structure and thermal instability of bovine mitochondrial tRNASerUGA investigated by proton NMR spectroscopy. *J. Mol. Biol.*, **284**, 57–69.
39. Hao,R., Zhao,M.W., Hao,Z.X., Yao,Y.N. and Wang,E.D. (2005) A T-stem slip in human mitochondrial tRNALeu(CUN) governs its charging capacity. *Nucleic Acids Res.*, **33**, 3606–3613.
40. Friederich,M.W., Gast,F.U., Vacano,E. and Hagerman,P.J. (1995) Determination of the angle between the anticodon and aminoacyl acceptor stems of yeast phenylalanyl tRNA in solution. *Proc. Natl Acad. Sci. USA*, **92**, 4803–4807.
41. Helm,M. and Attardi,G. (2004) Nuclear control of cloverleaf structure of human mitochondrial tRNA(Lys). *J. Mol. Biol.*, **337**, 545–560.
42. Ueda,T., Yotsumoto,Y., Ikeda,K. and Watanabe,K. (1992) The T-loop region of animal mitochondrial tRNA(Ser)(AGY) is a main recognition site for homologous seryl-tRNA synthetase. *Nucleic Acids Res.*, **20**, 2217–2222.
43. Shimada,N., Suzuki,T. and Watanabe,K. (2001) Dual mode recognition of two isoacceptor tRNAs by mammalian mitochondrial seryl-tRNA synthetase. *J. Biol. Chem.*, **276**, 46770–46778.
44. Levinger,L., Morl,M. and Florentz,C. (2004) Mitochondrial tRNA 3′ end metabolism and human disease. *Nucleic Acids Res.*, **32**, 5430–5441.
45. Levinger,L., Oestreich,I., Florentz,C. and Morl,M. (2004) A pathogenesis-associated mutation in human mitochondrial tRNALeu(UUR) leads to reduced 3′ end processing and CCA addition. *J. Mol. Biol.*, **337**, 535–544.
46. Rossmanith,W. and Karwan,R.M. (1998) Impairment of tRNA processing by point mutations in mitochondrial tRNA(Leu)(UUR) associated with mitochondrial diseases. *FEBS Lett.*, **433**, 269–274.
47. Yasukawa,T., Suzuki,T., Ishii,N., Ueda,T., Ohta,S. and Watanabe,K. (2000) Defect in modification at the anticodon wobble nucleotide of mitochondrial tRNA(Lys) with the MERRF encephalomyopathy pathogenic mutation. *FEBS Lett.*, **467**, 175–178.
48. Umeda,N., Suzuki,T., Yukawa,M., Ohya,Y., Shindo,H., Watanabe,K. and Suzuki,T. (2005) Mitochondria-specific RNA-modifying enzymes responsible for the biosynthesis of the wobble base in mitochondrial tRNAs. Implications for the molecular pathogenesis of human mitochondrial diseases. *J. Biol. Chem.*, **280**, 1613–1624.
49. Schneider,A. (1996) Cytosolic yeast tRNA(His) is covalently modified when imported into mitochondria of *Trypanosoma brucei*. *Nucleic Acids Res.*, **24**, 1225–1228.